Quantum Electronics **43** (12) 1110–1117 (2013)

INTERACTION OF LASER RADIATION WITH MATTER

PACS numbers: 32.80.Rm; 52.25.Os; 52.50.Jm
DOI: 10.1070/QE2013v043n12ABEH015238

Plasma channel produced by femtosecond laser pulses as a medium for amplifying electromagnetic radiation of the subterahertz frequency range

A.V. Bogatskaya, E.A. Volkova, A.M. Popov

Abstract. **The electron energy distribution function in the plasma channel produced by a femtosecond laser pulse with a wavelength of 248 nm in atmospheric-pressure gases was considered. Conditions were determined whereby this channel may be employed for amplifying electromagnetic waves up to the terahertz frequency range over the energy spectrum relaxation time $\sim 10^{-7}$ s. Gains were calculated as functions of time and radiation frequency. The effect of electron–electron collisions on the rate of relaxation processes in the plasma and on its ability to amplify the electromagnetic radiation was investigated.**

Keywords: *multiphoton ionisation, plasma channel, electromagnetic radiation amplification, electron energy distribution function.*

1. Introduction

An important feature inherent in the plasma objects emerging in the field of a femtosecond laser pulse is their strongly nonequilibrium character. This nonequilibrium character may be employed for several practical applications, in particular for generating VUV and soft X-ray radiation pulses of attosecond duration [1, 2]. When the laser pulse duration is shorter than or of the order of the inverse frequency of atomic collisions, the energy spectrum of the photoelectrons produced in the multiphoton ionisation of gases consists of a set of peaks corresponding to the absorption of a certain number of photons in the above-threshold ionisation. This electron energy distribution function (EEDF) has energy ranges which are actually characterised by population inversion; as is commonly known, this can be used for amplifying electromagnetic radiation in the plasma [3–5]. As noted in Ref. [4], first and foremost the amplification effect may occur in gases characterised by the electron energy range in which the transport scattering cross section increases with electron energy. In Ref. [6] it was shown that this kind of radiation amplification is possible in the radio frequency range in xenon plasmas produced by 248-nm radiation ($\hbar\Omega = 5$ eV) during the energy spectrum relaxation time. At atmospheric gas pressure and in the absence of electron–electron collisions this time was estimated at 100–200 ns.

In the present work we comprehensively analyse whether plasma channels produced by high-power ultrashort pulses (USPs) of the visible or UV frequency range in different atmospheric-pressure gases can be employed for amplifying radio-frequency radiation. Proceeding from the Boltzmann kinetic equation we analysed the temporal evolution of the electron energy spectrum in the relaxing plasma produced by the laser pulse; in doing this we took into account, in particular, electron–electron collisions. The gains for electromagnetic radiation in the plasma channel were calculated as functions of time and amplified radiation frequency. The conditions were determined whereby this relaxing plasma may be used as an efficient amplifying medium for radio-frequency radiation pulses, including pulses of the subterahertz frequency range.

A.V. Bogatskaya, A.M. Popov D.V. Skobel'tsyn Institute of Nuclear Physics, M.V. Lomonosov Moscow State University, Vorob'evy gory, 119991 Moscow, Russia; Department of Physics, M.V. Lomonosov Moscow State University, Vorob'evy gory, 119991 Moscow, Russia; e-mail: alexander.m.popov@gmail.com;
E.A. Volkova D.V. Skobel'tsyn Institute of Nuclear Physics, M.V. Lomonosov Moscow State University, Vorob'evy gory, 119991 Moscow, Russia

Received 23 May 2013; revision received 21 July 2013
Kvantovaya Elektronika **43** (12) 1110–1117 (2013)
Translated by E.N. Ragozin

2. Formulation of the problem

In the analysis of the properties and the evolution of the plasma channel produced by high-power femtosecond laser radiation it is well to keep in mind that the channel is formed only due to the multiphoton or tunnel ionisation of atoms or molecules, while the avalanche ionisation may be neglected. Furthermore, it turns out that elastic electron collisions with the atoms (molecules) of the medium may also be neglected during the course of the pulse. To be specific, we estimate the characteristic the electron–atom (molecule) collision time as $T_c \approx 1/(N\sigma v)$, where $N \simeq 3 \times 10^{19}$ cm^{-3} is the particle density at atmospheric pressure, $\sigma \simeq 10^{-15}$ cm^2 is the collision cross section, and $v \sim 10^8$ cm s^{-1} is the velocity of electrons resulting from photoionisation. Under these conditions, T_c is equal to $\sim 3 \times 10^{-13}$ s. This signifies that the photoelectron energy spectrum for a laser pulse no longer than 300 fs is determined only by the photoionisation dynamics of atoms (molecules) of the gas and may be derived by solving the problem of single atom (molecule) ionisation in a strong laser field. The electron spectrum evolution, which is described by the Boltzmann kinetic equation and is due to elastic and inelastic collisions with atoms (molecules) of the gas as well as by electron–electron collisions, takes place in the post-pulse regime. Under these conditions, the problem of gas ionisation by laser radiation and the problem of photoelectron spectrum evolution can therefore be treated independently of each other, the solution of the former problem being the initial condition for the latter.

In our work the spectrum dynamics of the photoelectrons produced by $\lambda = 248$ nm radiation, which corresponds to the photon energy $\hbar\Omega = 5$ eV of KrF excimer laser radiation, was investigated for rare gases (argon, xenon) and molecular nitrogen at atmospheric pressure. In this case, the existence of Ramsauer minimum of the transport cross section for scattering by rare-gas atoms may provide the necessary conditions for the emergence of electromagnetic radiation amplification in the gas. The cross section for electron scattering by nitrogen molecules also has an interval in which it increases with electron energy. However, the existence of low-lying vibrational states makes the EEDF evolution qualitatively different from that in rare gases.

The photoionisation dynamics was calculated by way of numerical integration of the Schrödinger equation for model single-electron atoms with ionisation potentials $I_i = 12.13$ and 15.76 eV equal to the ionisation potentials of xenon and argon atoms. The single-electron model of xenon atoms is similar to that employed in Ref. [7]. In the framework of this model the valence electron motion in a xenon atom is defined by the potential

$$V(r) = -\frac{e^2}{\sqrt{\beta^2 + r^2}}, \quad (1)$$

where the smoothing parameter $\beta = 0.0943$ Å is so selected that the ionisation potential is equal to that of xenon atoms. Similarly, argon atoms are modelled by the potential

$$V(r) = -\frac{e^2}{\sqrt{\beta^2 + r^2}}[1 + a\exp(-br)], \quad (2)$$

where $\beta = 0.0265$ Å; $a = 0.1$; $b = 0.2$ Å^{-1}. The ground state in potential (2) is characterised by the binding energy $I_i = 15.76$ eV, which corresponds to the ionisation potential of argon atoms. The ionisation potential of nitrogen molecules ($I_i = 15.58$ eV) is close to that of argon atoms. That is why the photoionisation probabilities of argon atoms and nitrogen molecules were assumed to be approximately equal and the peak positions in the photoelectron spectra were assumed to differ by a value equal to the difference in the ionisation potentials of Ar and N_2.

The envelope of the laser pulse was assumed to possess a smoothed $\sin^2$ shape with leading- and trailing-edge times t_f:

$$E_0(t) = E_0 \sin^2 \frac{\pi t}{2t_f}, \quad 0 \leqslant t \leqslant 2t_f, \quad (3)$$

where the field intensity amplitude E_0 is related to the radiation intensity, which is used below, by the formula $P = cE_0^2 \times (8\pi)^{-1}$. In our calculations we assumed that $t_f = 50T$ ($T = 2\pi/\Omega$ is the optical oscillation period); for $\hbar\Omega = 5$ eV the pulse duration $\tau_p = 2t_f \approx 75$ fs.

The method for numerical integration of the Schrödinger equation was discussed in detail in Ref. [8].

3. Photoionisation of gases by a laser USP

At first we dwell on the calculated photoionisation probabilities and photoelectron spectra produced by femtosecond laser pulses. Figure 1 shows the probabilities of ionisation (per pulse) of argon and xenon atoms. For intensities up to $P \sim 10^{14}$ W cm^{-2} the ionisation of xenon atoms is described by a cubic dependence on the radiation intensity, which corresponds to the third order of perturbation theory. As for argon atoms, the ionisation is a four-photon event described by the dependence $w_i \sim P^4$ up to $P < 3 \times 10^{13}$ W cm^{-2}. Observed in higher fields is the trend for saturation of the ionisation probability at a level well below unity, which is caused by trapping of atoms in highly excited states near the continuum boundary; these states are populated due to the existence of a three-photon resonance between the ground state and a group of Rydberg states (for more details, see Ref. [9]). In the case of ionisation of xenon atoms the like resonance is nonexistent, and no special features are observed in the $w_i(P)$ dependence. Figure 2 shows the typical photoelectron spectra produced in the photoionisation of xenon and argon atoms. For $P < 10^{13}$ W cm^{-2}, the Stark shift of the continuum boundary may be neglected, and therefore the position of the first peak in the xenon photoelectron spectrum will correspond to an energy $\varepsilon_0 = 3\hbar\Omega - I_i \approx 2.87$ eV; in this case, the probability of above-threshold absorption is negligible. A similar situation takes place for argon atoms. The photoelectron spectrum is dominated by the peak corresponding to the four-photon absorption with an energy $\varepsilon_0 = 4\hbar\Omega - I_i \approx 4.24$ eV, while the peaks corresponding to above-threshold absorption are small.

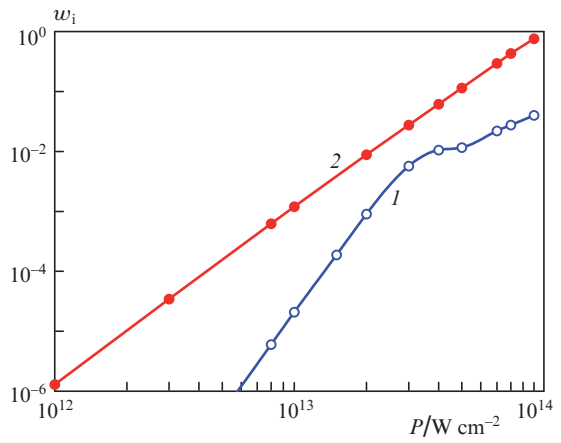

Figure 1. Ionisation probabilities w_i of argon (*1*) and xenon (*2*) atoms per pulse as functions of intensity P of laser radiation with $\lambda = 248$ nm.

Therefore, our analysis of the calculated data suggests the following conclusions. For the intensity range under consideration, a laser pulse duration $\tau_p \sim 75$ fs, and an atomic density $N \simeq 3 \times 10^{19}$ cm^{-3}, by the end of the laser pulse there forms a plasma channel in the volume defined by the parameters of the optical system, this channel being characterised by a peak energy spectrum structure and an ionisation degree $\alpha = N_e/N \approx 10^{-7} - 10^{-4}$ (N_e is the electron density) and over. In this case, the peak width $\Delta\varepsilon$ in the photoelectron spectrum is defined by the pulse duration and is equal to ~0.2 eV for a bandwidth-limited pulse.

4. Boltzmann kinetic equation for the photoelectron energy spectrum

The time evolution of the plasma object produced by a femtosecond pulse was investigated proceeding from the Boltzmann kinetic equation for the electron velocity distribution function $f(\boldsymbol{v}, t)$:

$$\frac{\partial f(\boldsymbol{v}, t)}{\partial t} - \frac{e\boldsymbol{E}}{m}\frac{\partial f}{\partial \boldsymbol{v}} = \mathrm{St}(f), \quad (4)$$

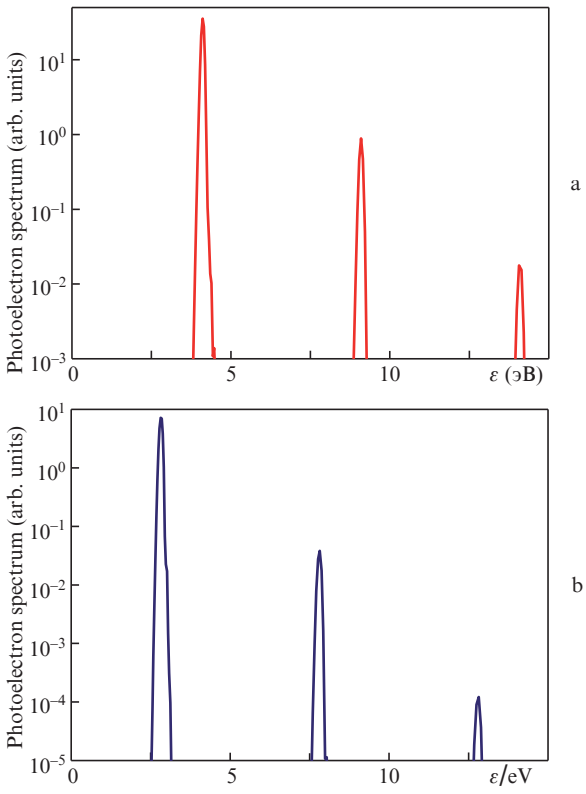

Figure 2. Photoelectron spectra in argon for a radiation intensity $P = 3 \times 10^{13}$ W cm^{-2} (a) and in xenon for $P = 10^{13}$ W cm^{-2} (b).

where $\boldsymbol{E} = \boldsymbol{E}_0 \cos\omega t$ is the intensity of the electric field of the radio-frequency radiation propagating through the plasma channel and $\mathrm{St}(f)$ is the collision integral. In the framework of a polynomial expansion the distribution function $f(\boldsymbol{v}, t)$ can be represented in the form

$$f(\boldsymbol{v}, t) = \sum_n f_n(v, t) P_n(\cos\theta), \tag{5}$$

where $P_n(\cos\theta)$ is the Legendre polynomial and θ is the angle between the velocity vector and the electric intensity $\boldsymbol{E}$ aligned with the z axis. Usually the anisotropy of velocity distribution is weak (for more details, see Refs [3, 5]), and series (5) is restricted to only two terms of expansion:

$$f(\boldsymbol{v}, t) = f_0(v, t) + f_1(v, t)\cos\theta, \tag{6}$$

where the isotropic part $f_0(v, t)$ of the distribution function describes the electron distribution over the velocity modulus and the small anisotropic addition $f_1(v, t)$ permits calculating the electric current (aligned with the z-axis) emerging in the plasma:

$$j_z(t) = -\frac{4\pi}{3} e N_e \int v^3 f_1(v, t)\,\mathrm{d}v. \tag{7}$$

By substituting expansion (6) in Eqn (4) it is easy to obtain the system of equations for the harmonics $f_0(v, t)$ and $f_1(v, t)$ of the distribution function:

$$\begin{aligned} &\frac{\partial f_0(v,t)}{\partial t} = \frac{eE(t)}{3mv^2}\frac{\partial}{\partial v}[v^2 f_1(v,t)] + Q, \\ &\frac{\partial f_1(v,t)}{\partial t} + \nu_{\mathrm{tr}} f_1(v,t) = \frac{eE(t)}{m}\frac{\partial f_0}{\partial v}. \end{aligned} \tag{8}$$

Here, $\nu_{\mathrm{tr}}(v) = N\sigma_{\mathrm{tr}} v$ and σ_{tr} are the transport frequency and scattering cross section;

$$Q = \frac{1}{4\pi}\int \mathrm{St}(f)\,\mathrm{d}\Omega;$$

and the function $f_0(v, t)$ is normalised according to the condition

$$4\pi \int f_0(v, t) v^2 \mathrm{d}v = 1. \tag{9}$$

From Eqns (8) it is easy to obtain [3] the following equation for the EEDF $n(\varepsilon, t)$:

$$\frac{\partial n(\varepsilon,t)}{\partial t}\sqrt{\varepsilon} = \frac{\partial}{\partial\varepsilon}\left[\frac{e^2 E_0^2 \nu_{\mathrm{tr}}(\varepsilon)}{3m(\omega^2 + \nu_{\mathrm{tr}}^2)}\varepsilon^{3/2}\frac{\partial n}{\partial\varepsilon}\right]$$

$$+\frac{2m}{M}\frac{\partial}{\partial\varepsilon}\left\{\nu_{\mathrm{tr}}(\varepsilon)\varepsilon^{3/2}\left[n(\varepsilon,t) + T_{\mathrm{g}}\frac{\partial n(\varepsilon,t)}{\partial\varepsilon}\right]\right\} + Q_{\mathrm{ee}}(n) + Q^*(n), \tag{10}$$

which in essence is the electron diffusion equation in energy space [3, 5]. Here, $\varepsilon = mv^2/2$; T_{g} is the gas temperature (in what follows we assume that $T_{\mathrm{g}} \approx 0.03$ eV); m is the electron mass; M is the mass of gas atom (or molecule); $Q_{\mathrm{ee}}(n)$ and $Q^*(n)$ are the electron–electron and inelastic collision integrals. The electron–electron collision integral is written in the form (see, for instance, Ref. [3])

$$Q_{\mathrm{ee}}(n) = \frac{\partial}{\partial\varepsilon}\left\{\nu_{\mathrm{ee}}(\varepsilon)\varepsilon^{3/2}\left[A_1(\varepsilon,t) + A_2(\varepsilon,t)\frac{\partial n}{\partial\varepsilon}\right]\right\}, \tag{11}$$

where ν_{ee} is the electron–electron collision frequency and the integral expressions for $A_1(\varepsilon, t)$ and $A_2(\varepsilon, t)$ are of the following form:

$$A_1(\varepsilon,t) = \int_0^\varepsilon n(\varepsilon,t)\sqrt{\varepsilon}\,\mathrm{d}\varepsilon,$$

$$A_2(\varepsilon,t) = \frac{3}{2}\left[\int_0^\varepsilon n(\varepsilon,t)\varepsilon^{3/2}\mathrm{d}\varepsilon + \varepsilon^{3/2}\int_\varepsilon^\infty n(\varepsilon,t)\mathrm{d}\varepsilon\right].$$

The inelastic collision integral

$$Q^*(n) = \sum_i [-\nu_i^*(\varepsilon) n(\varepsilon,t)\sqrt{\varepsilon}$$

$$+\nu_i^*(\varepsilon + I_i^*) n(\varepsilon + I_i^*, t)\sqrt{\varepsilon + I_i^*}], \tag{12}$$

where $\nu_i^* = N\sigma_i^*(\varepsilon)\sqrt{2\varepsilon/m}$ and σ_i^* are the frequency and cross section for the excitation of the ith inelastic state with the excitation threshold I_i^*, and summation in expression (12) is performed over all inelastic processes.

In the analysis of the evolution of the energy spectrum we assume that the plasma channel is produced at the initial (zero) instant of time, which corresponds to the end of the laser pulse, and that the plasma channel has a given degree of ionisation and a strongly nonequilibrium EEDF, which is subsequently approximated by a Gaussian function:

$$n(\varepsilon, t = 0) = \frac{1}{\Delta\varepsilon\sqrt{\pi\varepsilon}}\exp\left[-\frac{(\varepsilon - \varepsilon_0)^2}{\Delta\varepsilon^2}\right]. \tag{13}$$

The given EEDF is normalised according to the condition

$$\int_0^\infty n(\varepsilon, t = 0)\sqrt{\varepsilon}\,\mathrm{d}\varepsilon = 1, \tag{14}$$

and the quantity $n(\varepsilon, t)\sqrt{\varepsilon}$ is the probability density to find an electron with an energy ε.

In this work we also assume that the electromagnetic field of frequency ω, which propagates through the plasma channel, is weak and has no effect on the time evolution of the EEDF.

In rare gases, the energy-lowest excitation thresholds for electronic states are equal to 8.31 eV for xenon atoms and 11.5 eV for argon atoms. This is significantly higher than the energy peak corresponding to the photoelectrons produced by the femtosecond laser pulse. Under the conditions involved, the spectrum evolution in the rare gases is therefore determined only by elastic and electron–electron collisions. As for the EEDF evolution for molecular nitrogen, account should also be taken of low-lying vibrational states, which are characterised by large electron collisional excitation cross sections in the ~2–4 eV energy range and which substantially speed up the EEDF relaxation.

Equation (10) subject to initial condition (13) was numerically solved with the use of a Galerkin procedure, with trial function approximation by the finite-element method [10] in the energy range $\varepsilon = 0-10$ eV. The integration steps in time and energy were equal to 10^{-13} s and 10^{-2} eV, the total computation time amounted to 300 ns, depending on the conditions of the problem at hand. The cross sections of the elementary processes for xenon were taken from Refs [11, 12], for argon from Ref. [13], and for nitrogen from Refs [14, 15].

Figure 3 depicts the transport cross sections for argon and xenon. A characteristic feature of these cross sections is the existence of Ramsauer minimum and the portion with a positive value of the derivative $d\sigma_{tr}/d\varepsilon$ in energy ranges of 0.25–11.0 eV in argon and 0.64–5.0 eV in xenon. In the energy range below 2.2 eV, the transport cross section for argon is also characterised by positive values of the derivative $d\sigma_{tr}/d\varepsilon$ (Fig. 4).

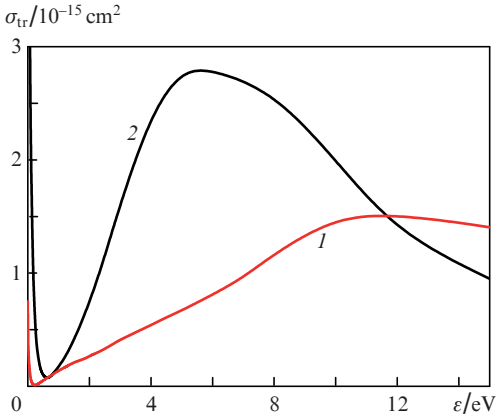

Figure 3. Transport cross sections for electron scattering from argon (*1*) and xenon (*2*) atoms.

5. Amplification of electromagnetic radiation in the plasma channel with a strongly nonequilibrium EEDF

As noted above, the authors of Refs [5, 6] discussed the feasibility of amplifying electromagnetic radiation in plasma channels with an EEDF having an energy range with a population inversion. In fact, the expression for the complex conductance $\sigma(\omega) = \sigma'(\omega) + i\sigma''(\omega)$ at a frequency ω is readily

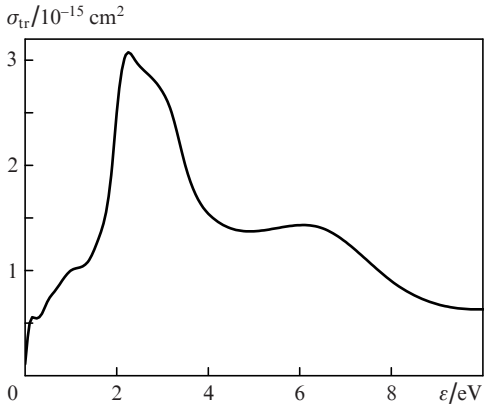

Figure 4. Transport cross section for electron scattering from nitrogen molecules.

found from expressions (7), (8) and may be written as (see, for instance, Refs [3, 5])

$$\sigma(\omega) = \frac{2}{3}\frac{e^2 N_e}{m}\int_0^\infty \frac{\varepsilon^{3/2}[\nu_{tr}(\varepsilon) + i\omega]}{\omega^2 + \nu_{tr}^2(\varepsilon)}\left[-\frac{\partial n(\varepsilon, t)}{\partial \varepsilon}\right]d\varepsilon. \qquad (15)$$

The real part of this expression describes the dissipation of electromagnetic wave energy in the plasma, and it is easy to obtain the relation for the absorption coefficient at a frequency ω:

$$\mu_\omega = \frac{4\pi\sigma'}{c} = \frac{8\pi}{3}\frac{e^2 N_e}{mc}\int_0^\infty \frac{\varepsilon^{3/2}\nu_{tr}(\varepsilon)}{\omega^2 + \nu_{tr}^2(\varepsilon)}\left[-\frac{\partial n(\varepsilon, t)}{\partial \varepsilon}\right]d\varepsilon. \qquad (16)$$

The EEDF usually decreases with increase in energy, i.e. $\partial n/\partial\varepsilon < 0$, and therefore the value of integral (16) is positive: $\sigma' > 0$ and $\mu_\omega > 0$. However, the electron energy distribution which emerges in the course of gas photoionisation by a laser USP necessarily contains domains where $\partial n/\partial\varepsilon > 0$. These domains make a negative contribution to integral (16) and the absorption coefficient becomes lower. The authors of Refs [4, 6] drew attention to the following fact: in the low-frequency domain corresponding to the condition $\omega < \nu_{tr}$ (for the atmospheric-pressure gases under consideration, this condition is fulfilled even in the subterahertz frequency range $\omega \leqslant 10^{12}$ s^{-1}), integral (16) may turn out to be negative for the distribution function of the form (13) for gases with a strongly pronounced Ramsauer effect. In this situation the medium will be capable of amplifying radio-frequency radiation. Specifically, from relation (16) we obtain the necessary condition for signal amplification:

$$\frac{d}{d\varepsilon}\left[\frac{\varepsilon^{3/2}\nu_{tr}(\varepsilon)}{\omega^2 + \nu_{tr}^2(\varepsilon)}\right] < 0, \qquad (17)$$

which should be fulfilled in the existence domain of a photonisation peak. When $\omega \ll \nu_{tr}$, from inequality (17), in view of the expression $\nu_{tr} \sim \sqrt{\varepsilon}\,\sigma_{tr}(\varepsilon)$, we have

$$\frac{d}{d\varepsilon}\left[\frac{\varepsilon}{\sigma_{tr}(\varepsilon)}\right] < 0, \qquad (18)$$

i.e. the transport cross section $\sigma_{tr}(\varepsilon)$ must grow with energy faster than ε. The dependences $\varepsilon/\sigma_{tr}(\varepsilon)$ are plotted in Fig. 5 for the gases investigated in our work. These data show that the

onset of amplification in the photoionisation plasma produced by $\lambda = 248$ nm radiation may be expected primarily in xenon and molecular nitrogen. At the same time, for argon in the energy domain $0.8 < \varepsilon < 10$ eV the quantity $\varepsilon/\sigma_{tr}(\varepsilon)$ is practically constant, i.e. the amplification effect may occur only for slow electrons in a narrow energy range ($\varepsilon = 0.6$–0.8 eV), which is supposedly hard to realise experimentally.

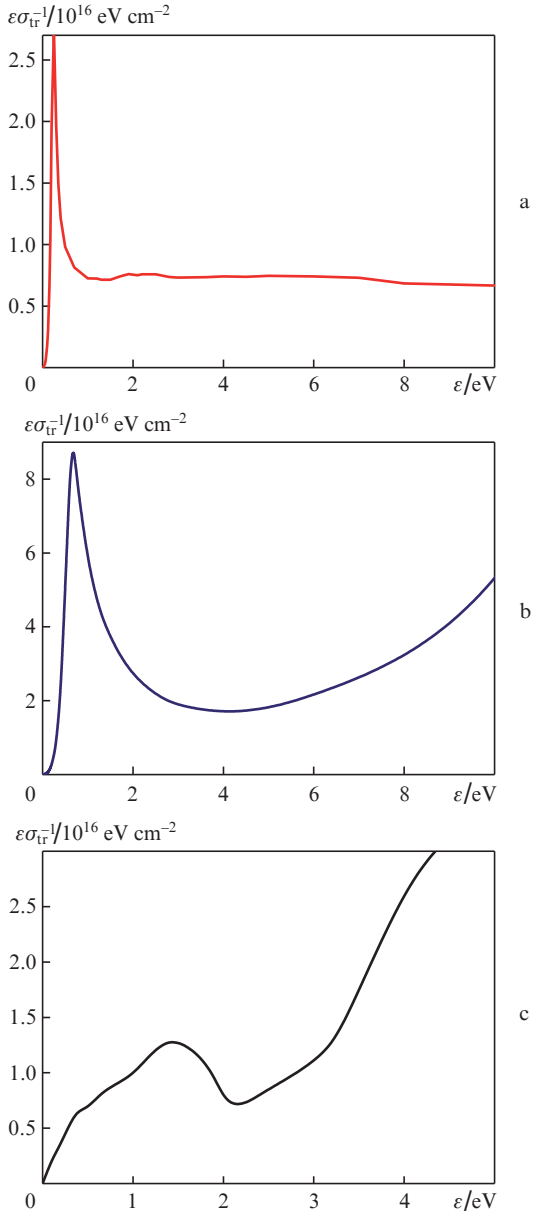

Figure 5. ε/σ_{tr} as a function of electron energy for argon (a), xenon (b), and nitrogen (c).

Under conditions where the evolution of the electron energy spectrum proceeds only due to their elastic collisions with neutral atoms, the characteristic EEDF relaxation time may be estimated as

$$\tau_\varepsilon \approx \frac{M}{2m}\nu_{tr}^{-1}. \qquad (19)$$

In our calculations an estimate of formula (19) yields $\tau_\varepsilon \approx 10^{-7}$ s. This signifies that the effect of electromagnetic radiation amplification in the plasma may be expected during precisely this period of time. The plasma channel in xenon produced by femtosecond laser radiation at a wavelength $\lambda = 248$ nm will therefore be capable of amplifying radio-frequency pulses (up to the terahertz frequency range) several tens of nanoseconds in duration. In the case of molecular nitrogen the situation is more complicated. On the one hand, the energy range where the amplification effect may be expected is rather narrow and amounts to only 1.5–2.0 eV. On the other hand, what is more important, the energy spectrum relaxation in this energy range proceeds primarily due to vibrational excitation of nitrogen molecules and is characterised by the time

$$\tau^* \approx \frac{\varepsilon}{I_v}(\nu^*)^{-1}, \qquad (20)$$

where $I_v = 0.29$ eV is the vibrational quantum of the nitrogen molecule; and $\nu^* = N\sigma_v\sqrt{2\varepsilon/m}$ and σ_v are the frequency and cross section for the excitation of the vibrational state $N_2(X^1\Sigma, v = 1)$. Assuming that $\varepsilon = 2$ eV and $\sigma_v \approx 10^{-16}$ cm^2, from formula (20) we obtain $\tau^* \approx 3 \times 10^{-11}$ s, which is three orders of magnitude shorter than in rare gases. This actually signifies that the plasma channel produced in molecular gas medium is hardly applicable for amplifying radio-frequency radiation.

Numerical calculations confirm our estimates. Figure 6 shows the EEDF data calculated on the basis of Eqn (10) neglecting electron–electron collisions in argon and xenon at different instants of time. One can see that the EEDF possesses a strongly pronounced peak throughout the simulation time interval (200 ns); the peak position gradually shifts to

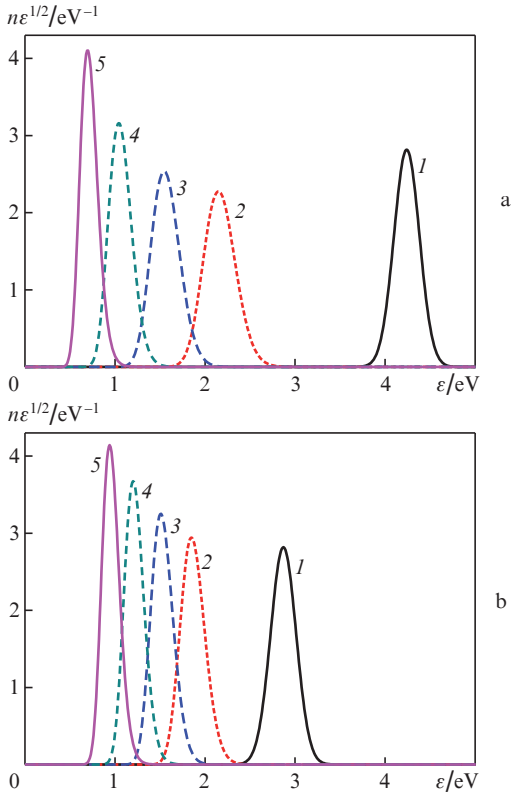

Figure 6. EEDF for argon (a) and xenon (b) at the points in time $t = (1)$ 0, (2) 25, (3) 50, (4) 100, and (5) 200 ns after plasma channel production by $\lambda = 248$ nm laser radiation.

lower energies, the diffusive spreading of the spectrum in energy space being negligible. Furthermore, the lowering of elastic collision frequency ν_{tr} with the slowing-down of electrons leads to the opposite effect – the narrowing of the peak in the photoelectron spectrum. Figure 7 shows the time dependences of spectrum-averaged photoelectron energy

$$\langle\varepsilon(t)\rangle = \int_0^\infty n(\varepsilon,t)\varepsilon^{3/2}\mathrm{d}\varepsilon \qquad (21)$$

which also indicates a siginificant slowdown of electron cooling with time.

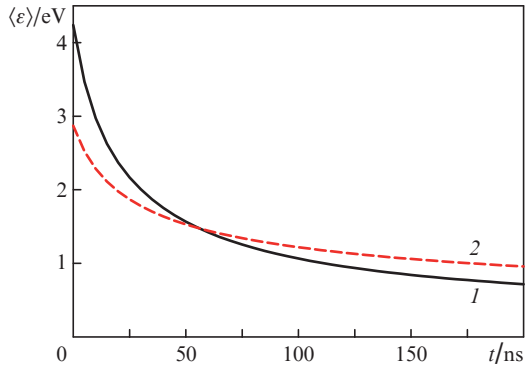

Figure 7. Time dependences of the spectrum-averaged photoelectron energy in argon (*1*) and xenon (*2*) plasmas.

A qualitatively different situation occurs in molecular nitrogen (Fig. 8). In this case, the time EEDF evolution is primarily determined by the energy dependence of the cross sections for the vibrational excitation of the nitrogen molecule, which have a maximum in the 2–4 eV energy range. As a result, the initial peak in the ~4.4 eV domain vanishes in a time of $\sim 10^{-11}$ and shifts to an energy domain near 1.5 eV, in which the collisional excitation cross section is small ($\sim 10^{-17}$ cm^2) and the effect of collisional excitation of nitrogen molecules on the EEDF is therefore not so significant. Comparing the data given in Figs 8 and 5c shows that the plasma channel in nitrogen also cannot be employed for the amplification of radio-frequency radiation, including the 10^{-11}–10^{-10} s time range.

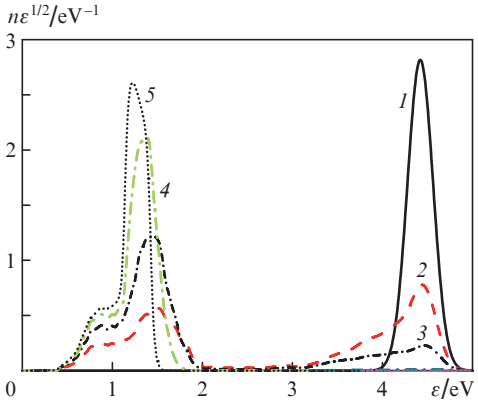

Figure 8. EEDF for molecular nitrogen at the points in time t = (*1*) 0, (*2*) 25, (*3*) 50, (*4*) 100, and (5) 200 ns after plasma channel production by λ = 248 nm laser radiation.

The calculated EEDFs were employed for calculating the electromagnetic radiation gain in the plasma. These calculations demonstrate the validity of the above hypothesis that amplification is possible to occur only in xenon plasmas. For plasma channels in argon or nitrogen, attempts to make the gain positive do not meet with success. Figure 9 shows the calculated gain $k_\omega = -\mu_\omega$ in the xenon plasma channel for an electron density $N_e = 10^{10}$ cm^{-3} and different frequencies of amplified radiation. The highest gain is achieved for the lowest radiation frequency ($\omega = 10^{11}$ s^{-1}). In this case, in the process of energy spectrum relaxation for $t \leqslant 100$ ns we observed an increase in k_ω caused by the lowering of the transport cross section in the energy range which makes the most significant contribution to integral (16). With increase in radiation frequency ω the highest value of the gain k_ω shows a tendency for a decrease, with a simultaneous narrowing of the time interval during which the gain is positive. This circumstance is due to the following fact: in the process of EEDF relaxation, with increase in amplified radiation frequency the condition $\nu_{tr}(\varepsilon) > \omega$ is violated for shorter times.

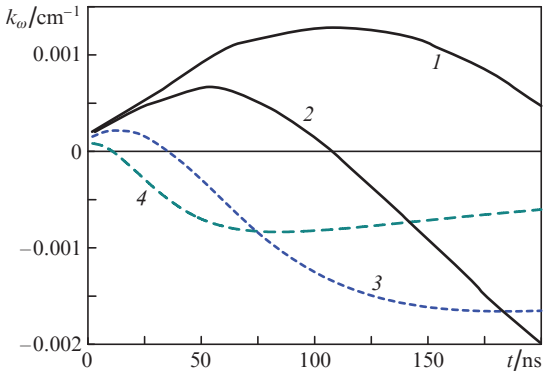

Figure 9. Electromagnetic radiation gains in the xenon plasma channel as functions of time for electromagnetic radiation frequencies ω = (*1*) 10^{11}, (*2*) 2×10^{11}, (*3*) 5×10^{11}, and (*4*) 10^{12} s^{-1}. Negative values correspond to absorption of the electromagnetic radiation in the plasma. The calculations were performed for a density $N = 2.5\times10^{19}$ cm^{-3} of neutral atoms and an electron density $N_e = 10^{10}$ cm^{-3}.

In the framework of our assumptions the gain [see expression (16)] turns out to be proportional to the degree of plasma ionisation, and therefore, on the face of it, raising the gain requires increasing the intensity of ionising laser radiation should. It is well known, however, that electron–electron collisions are favourable to a faster Maxwellisation of the photoelectron spectrum and, as a consequence, to disappearance of the amplification effect. In the presence of only elastic collisions, electron–electron collisions begin to exert a significant effect on the evolution of the energy spectrum in the plasma provided that

$$\alpha \sim \frac{2m}{M}\frac{\sigma_{tr}}{\sigma_{ee}}, \qquad (22)$$

where $\sigma_{ee}(\varepsilon) = (\pi\varepsilon^4/\varepsilon^2)L(\varepsilon)$ is the cross section for electron–electron (Coulomb) collisions and $L(\varepsilon)$ is the Coulomb logarithm, which is a smooth function of the energy. Putting $L \approx 1$, we obtain that in the energy domain $\varepsilon \approx 2$ eV, which corresponds to the peak position in the photoelectron spectrum, condition (22) is fulfilled for $\alpha \approx 5\times10^{-7}$, or $N_e \approx 10^{13}$ cm^{-3}.

Numerical simulations confirm our estimates. The results of numerical solution of the Boltzmann equation depicted in Fig. 10 suggest that the inclusion of electron–electron collisions has a significant effect on the EEDF evolution* even for an electron density $N_e = 10^{12}$ cm^{-3}, and for $N_e = 10^{13}$ cm^{-3} and $t \sim 200$ ns there occurs Maxwellisation of the spectrum. As is evident from the calculations, electron–electron collisions, in fact, significantly increase the electron diffusion coefficient in energy space, which is responsible for a rapid spreading of the photoelectron peak and the consequential narrowing of the time interval during which the gain in the channel is positive. Specifically, the data given in Fig. 11 show that the coefficient k_ω increases proportionally to the electron density in the channel; however, this dependence is realised over a time shorter than the energy spectrum relaxation time defined by the efficiency of electron–electron collisions. Increasing the electron density speeds up the EEDF relaxation, which shortens the period of the existence of a positive gain in the plasma. For instance, for an electron density of $\sim 10^{13}$ cm^{-3} in the channel, the gain k_ω amounts to ~ 0.3 cm^{-1} and a positive gain exists for ~ 20 ns. For $N_e = 10^{12}$ cm^{-3} we have $k_\omega \approx 0.05$ cm^{-1} and the amplification time $t \sim 100$ ns.

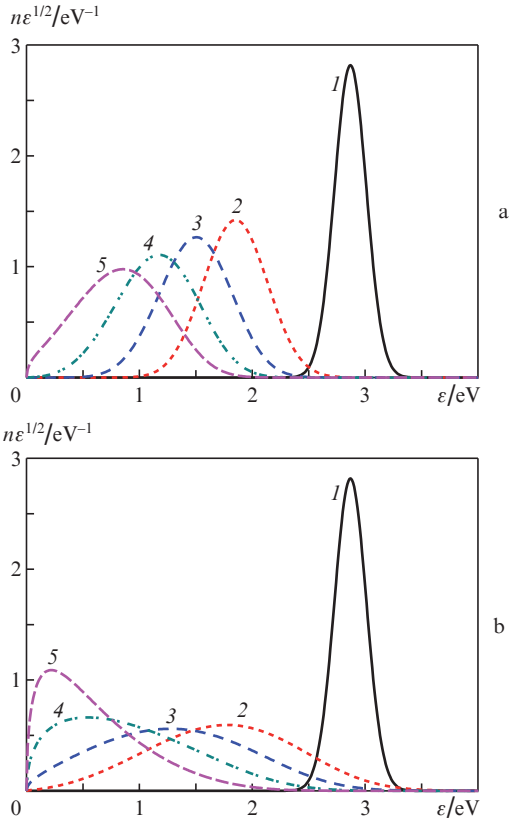

Figure 10. EEDF for xenon at the points in time $t = (1)$ 0, (2) 25, (3) 50, (4) 100, and (5) 200 ns after plasma channel production by $\lambda =$ 248 nm radiation. These calculations were carried out with the inclusion of electron–electron collisions for (a) $N_e = 10^{12}$ and (b) 10^{13} cm^{-3}.

*A comparison of the data obtained in the present work with the data of Ref. [6], which were calculated neglecting electron–electron collisions for the specified electron density $N_e = 10^{12}$ cm^{-3}, suggests, in particular, that the duration of the existence of a positive gain decreases twofold.

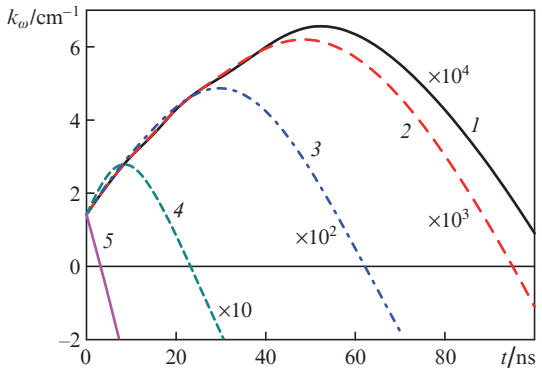

Figure 11. Electromagnetic radiation gains in the xenon plasma channel as functions of time for electron densities $N_e = (1)$ 10^{10}, (2) 10^{11}, (3) 10^{12}, (4) 10^{13}, and (5) 10^{14} cm^{-3}. These simulations were performed with the inclusion of electron–electron collisions for a density $N = 2.5 \times 10^{19}$ cm^{-3} of neutral atoms and an electromagnetic radiation frequency $\omega = 2 \times 10^{11}$ s^{-1}.

So far in the analysis of electromagnetic radiation in the plasma channel we assumed that the amplified radiation itself is weak and has no effect on the EEDF. This approach is obviously correct when the electron energy diffusion coefficient caused by the existence of the field under amplification is smaller than the diffusion coefficient in energy space defined by elastic electron collisions with gas atoms (molecules) as well as electron–electron collisions. We estimate the electron diffusion coefficient caused by the existence of radiofrequency radiation in the plasma (we assume that $\omega \ll \nu_{tr}$) as $D_\omega \sim e^2 E_0^2 \varepsilon/(3m\nu_{tr})$ and conclude that our treatment is correct when

$$\frac{e^2 E_0^2}{3m\nu_{tr}^2} \ll \max\left(\frac{2m}{M} T_g, \langle\varepsilon\rangle \frac{\nu_{ee}}{\nu_{tr}}\right). \qquad (23)$$

For instance, for xenon atoms, $\langle\varepsilon\rangle \approx 2$ eV, $T_g = 300$ K and an electron density $N_e = 10^{13}$ cm^{-3}, condition (23) is fulfilled when the intensity of radiofrequency radiation is lower than 10^3 W cm^{-2}.

In conclusion of this Section, we note that the amplification of the high-frequency radiation with $\omega \gg \nu_{tr}$, from the theoretical point of view, is also possible in a plasma channel with a nonmonotonic EEDF. In this case, as follows from relation (16), to achieve the amplification regime requires that the condition

$$\frac{\mathrm{d}}{\mathrm{d}\varepsilon}[\varepsilon^2 \sigma_{tr}(\varepsilon)] < 0 \qquad (24)$$

be fulfilled in the domain of peak location in the photoelectron spectrum, i.e. that the transport cross section should decrease with energy faster than ε^2. As discussed in Ref. [4], this type of the $\sigma_{tr}(\varepsilon)$ dependence is not typical for the known gases. Most likely it is valid to say that there is no gaseous medium with the properties required for the amplification of high-frequency radiation.

The effect of electromagnetic radiation amplification in the plasma channel produced in the ionisation of gas by a laser USP, which is considered in our work, is physically close to the effect of absolute negative conduction in a gas discharge plasma predicted in Refs [16, 17], discovered experimentally in Ref. [18], and discussed at length in Refs [19, 20]. A negative value of absolute conductivity signifies that the

electron gas is integrally moving in the direction of the field intensity vector of electromagnetic wave*. The physical cause for the emergence of absolute negative conduction is comprehensively discussed in Ref. [20]; it is due to the fact that the electrons accelerated by the field experience more frequent collisions than the electrons slowed down by the applied field. As a result, these field-decelerated electrons make the main electron contribution to the current emerging in the plasma. In this case, the conductivity considered as the coefficient of proportionality between the current density and the applied field turns out to be negative. A similar situation also takes place in the case of the oscillating electric field.

We would also like to emphasise that the effect of negative conduction in plasmas may be of interest in the problems of radiofrequency electromagnetic radiation propagation in the plasma waveguides produced by femtosecond laser pulses [21, 22]. Specifically, the permittivity of a plasma medium is related to the complex conductivity by the equation $\zeta = \zeta' + i\zeta'' = 1 + i4\pi\sigma/\omega$. Since the complex refractive index is $\sqrt{\zeta}$, the features of photoelectron energy spectrum evolution considered in our work may turn out to be significant also in studies of the optical properties of plasma waveguides.

6. Conclusions

Therefore, in this work we showed that the plasma channel produced by the radiation of a high-power laser USP in a dense gas and characterised by the presence of a rather narrow peak in the photoelectron spectrum may be employed for amplifying radio-frequency pulses, including pulses of the subterahertz frequency range. To achieve the maximum effect, for a working medium use should be made of the atomic gas in which the transport scattering cross section is characterised by the greatest value of the derivative $d\sigma_{tr}/d\varepsilon$ in the energy range corresponding to the photoelectron peak. It was shown that the gain may amount to a fraction of inverse centimetre for $t < 100$ ns.

Acknowledgements. The authors express their appreciation to participants of the seminar of the Division of Quantum Radiophysics at the P.N. Lebedev Physics Institute for helpful discussions. The Schrödinger equation was numerically integrated on the SKIF-MGU Chebyshev supercomputer.

This work was supported by the Russian Foundation for Basic Research (Grant No. 12-02-00064) and Dinastiya Nonprofit Foundation (Programme for the Support of Students Specialising in the Area of Theoretical Physics).

References

1. Agostini P., DiMauro L.F. *Rep. Prog. Phys.*, **67**, 813 (2004).
2. Krausz F., Ivanov M. *Rev. Mod. Phys.*, **81**, 163 (2009).
3. Ginzburg V.L., Gurevich A.V. *Usp. Fiz. Nauk*, **70**, 201 (1960).
4. Bunkin F.V., Kazakov A.E., Fedorov M.V. *Usp. Fiz. Nauk*, **107**, 559 (1972).
5. Raizer Yu.P. *Laser-Induced Discharge Phenomena* (New York: Consultants Bureau, 1977; Moscow: Nauka, 1974).
6. Bogatskaya A.V., Popov A.M. *Pis'ma Zh. Eksp. Teor. Fiz.*, **97**, 453 (2013).
7. Azarm A., Sharifi S.M., Sridharan A., Hosseini S., Wang Q.Q., Popov A.M., Tikhonova O.V., Volkova E.A., Chin S.L. *J. Phys. Conf. Ser.*, **414**, 012015 (2013).
8. Popov A.M., Tikhonova O.V., Volkova E.A. *Laser Phys.*, **21**, 1593 (2011).
9. Fedorov M.V., Poluektov N.P., Popov A.M., Tikhonova O.V., Kharin V.Yu., Volkova E.A. *IEEE J. Sel. Top. Quantum Electron.*, **18**, 42 (2012).
10. Fletcher C.A.J. *Computational Galerkin Methods* (New York: Springer-Verlag, 1984; Moscow: Mir, 1988).
11. Hayashi M. *J. Phys. D*, **16**, 581 (1983).
12. *Bibliography of Electron and Photon Cross Sections with Atoms and Molecules Published in the 20th Century–Xenon. Research Report NIFS-Data Series NIFS-DATA-79* (National Institute for Fusion Research, 2003).
13. Phelps A.V. *JILA Information Center Report No. 28* (Boulder, USA, University of Colorado, 1985).
14. Phelps A.V., Pitchford L.C. *Phys. Rev. A*, **31**, 2932 (1985).
15. Phelps A.V. *JILA Information Center Report No. 26* (Boulder, USA, University of Colorado, 1985).
16. Rokhlenko A.V. *Zh. Eksp. Teor. Fiz.*, **75**, 1315 (1978).
17. Shizgal S., McMahon D.R.A. *Phys. Rev. A*, **32**, 3669 (1985).
18. Warman J.M., Sowada U., DeHaas M.P. *Phys. Rev. A*, **31**, 1974 (1985).
19. Aleksandrov N.L., Napartovich A.P. *Usp. Fiz. Nauk*, **163**, 1 (1993).
20. Dyatko N.A. *J. Phys. Conf. Ser.*, **71**, 012005 (2007).
21. Zvorykin V.D., Levchenko A.O., Molchanov A.G., Smetanin I.V., Ustinovskii N.N. *Kratk. Soobshch. Fiz.*, (2), 49 (2010).
22. Zvorykin V.D., Levchenko A.O., Shutov A.V., Solomina E.V., Ustinovsky N.N., Smetanin I.V. *Phys. Plasmas*, **19**, 033509 (2012).

* Since the electron charge is negative, electrons usually move in the opposite direction to the electric field intensity vector.